Quantum Interference and Ballistic Transmission in Nanotube Electron Waveguides

Jing Kong, Erhan Yenilmez, Thomas W. Tombler, Woong Kim, and Hongjie Dai

Department of Chemistry and Laboratory for Advanced Materials, Stanford University, Stanford, California 94305

Robert B. Laughlin

Department of Physics, Stanford University, Stanford, California 94305

Lei Liu, C. S. Jayanthi, and S. Y. Wu

Department of Physics, University of Louisville, Louisville, Kentucky 40292

The electron transport properties of well-contacted individual single-walled carbon nanotubes are investigated in the ballistic regime. Phase coherent transport and electron interference manifest as conductance fluctuations as a function of Fermi energy. Resonance with standing waves in finite-length tubes and localized states due to imperfections are observed for various Fermi energies. Two units of quantum conductance $2G_0 = 4e^2/h$ are measured for the first time, corresponding to the maximum conductance limit for ballistic transport in two channels of a nanotube.

Electron transport behavior in single-walled carbon nanotubes (SWNT) is of fundamental and practical interest [1]. With ideal electrical contacts and two channels available for electron transport in a metallic SWNT, perfect transmission through the nanotube will manifest as two units of quantum conductance $G = 2G_0 = 4e^2/h$ (resistance $R = h/4e^2 = 6.45$ kΩ) by the system [1,2]. Individual SWNT samples with high contact resistance exhibit Coulomb blockade (CB) [3,4] and Luttinger liquid (LL) behavior [5] at various temperatures. Samples with low contact resistance are essential to investigating transport phenomena in SWNTs in the high transmission regime. Ballistic transport has been reported in only one channel of multiwalled nanotubes (MWNT) with $G = G_0 = 2e^2/h$ [6]. A possible explanation proposed by theory is that only the π^* channel allows for electron transport, as the π channel is being turned off due to substantial band shift caused by charge transfer between the MWNT and a jellium metal contact [7]. For SWNTs, transport measurements have observed conductance $G = T \times 2G_0 = 4Te^2/h$ with transmission probability up to $T \sim 0.5$−0.6 [8–10].

In this Letter, we present transport data obtained with samples of individual metallic SWNTs with highly transparent contacts $T \sim 1$. An important feature of these samples is that they show higher overall conductance at lower temperatures, as expected for metallic systems. This is rarely the case for most nanotube samples due to contact issues. Samples that exhibit CB [3,4], LL [5], and Kondo effect [10] exhibit lowered conductance at low temperatures. This work finds that for titanium contacted [11] metallic SWNTs, a fraction of them show negative $dG(T)/dT$ behavior. At low temperature, $2G_0 = 4e^2/h$ ($T \approx 1$) is measured with these samples, which reaches the maximum conductance limit of ballistic transport in two channels of a SWNT. Phase coherent

electron transport, confined standing waves, and localized states in the nanotubes lead to Fermi energy dependent quantum interference and resonance phenomena.

Sample preparation for individual SWNT electrical devices with titanium metal contacts is as reported previously [9]. The sample shown in Fig. 1 consists of a SWNT with diameter $\sim$1.5 nm and length $\sim$200 $\pm$ 10 nm (Fig. 1a inset). At room temperature, it shows a conductance of $1.1G_0$ ($R = 11$ kΩ) in regimes I and III of the conductance (G) vs gate-voltage (V_g) spectrum (Fig. 1a). A conductance dip is seen in regime II (Fig. 1a).

The overall conductance of the sample increases as temperature decreases. At low temperatures, conductance fluctuations vs V_g appear and the conductance peaks approach the quantum limit $2G_0 = 4e^2/h$ (Fig. 1). In regime II, the fluctuations are more drastic than in regimes I and III. Rapid conductance oscillations superimposed on slower fluctuations are also seen in regimes I and III (Figs. 1 and 2), but are absent in regime II. These conductance fluctuation features are highly reproducible in repeated measurements during the same experimental thermal cycle. For different cycles, the details of the slow fluctuations can vary (Fig. 1a vs 1b).

The conductance fluctuations vs Fermi energy and the peak conductance approaching $4e^2/h$ are our main results. We first discuss the origin of the fluctuations. The data in Fig. 1 differ from CB behavior of samples with high resistance metal-tube contacts (low conductance $T \sim 0.001$−0.01). The contacts in our sample are highly transparent approaching $T \sim 1$. The data are also inconsistent with CB in the strong tunneling regime, for which the overall conductance should decrease with temperature due to CB suppression [12]. In our case, the overall background conductance increases at lower temperatures.

We attribute the conductance fluctuations to interference or resonance phenomena [13–17] in 1D
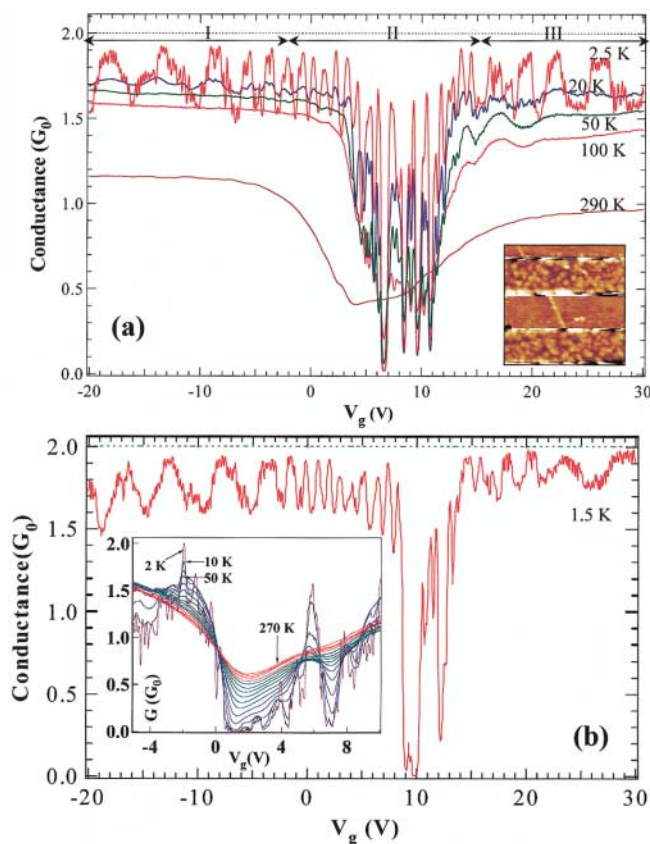
FIG. 1 (color). Quantum interference in a nanotube electron wave guide. (a) Conductance vs gate voltage recorded under a dc bias of 1 mV at various temperatures with a SWNT sample shown in the inset. The various gate-voltage regimes (I, II, and III) are marked. (b) Conductance vs gate voltage recorded with the same sample at 1.5 K but in a different thermal cycle than (a). Inset: Data recorded with a second metallic SWNT sample (diameter ~1.5 nm, length between electrodes ~800 nm) in the temperature range of 270–2 K.
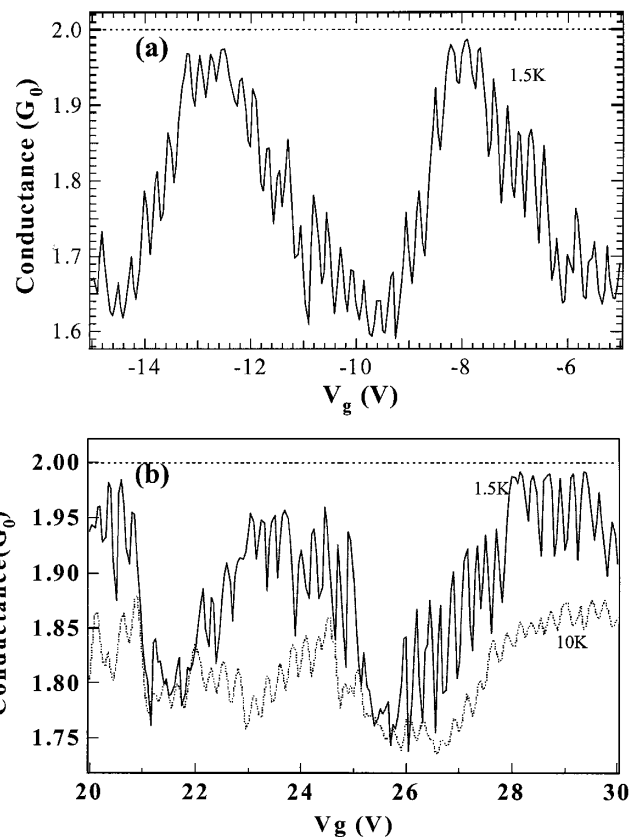

FIG. 2. Resonance effect due to standing waves. (a) Rapid quasiperiodic conductance oscillations over a slow fluctuation background observed in regime I of Fig. 1b at 1.5 K. (b) Rapid conductance oscillations observed in regime III at 1.5 K (solid line) and 10 K (dotted line), respectively.

manifested by the SWNT sample with transparent contacts. In regimes I and III, the rapid conductance oscillations are quasiperiodic with $\Delta V_g \sim 200$ meV (Fig. 2), and are attributed to resonance with standing waves [18] in the 200 nm long tube. The energies of standing waves are quantized with an expected spacing $\Delta E \sim (dE/dk)\Delta k = h\nu_F/2L \sim 10$ meV for $L \sim$ 200 nm and Fermi velocity $\nu_F \sim 8 \times 10^5$ m/s [18]. This spacing matches the period of the rapid conductance oscillations converted to energy ($\alpha \Delta V_g \sim 0.05 \times 200$ meV, where $\alpha \sim 0.05$ is the typical gate efficiency factor for our sample structures [19]). To our knowledge, this is the first time that resonance transport with standing waves is observed in SWNTs in the $T \sim 1$ regime. Notably, in ballistic channels of 2D electron gas systems, similar phenomena have been seen as conductance oscillations existing over quantized staircases [13,14].

The rapid conductance oscillations are over a slower fluctuation background in regimes I and III. The slower fluctuations become dramatic in regime II (Fig. 3a). The origin of the slow fluctuations is attributed to resonance scattering by localized states in the nanotube, and the manifestation of the localized states is energy (gate) dependent. It is known that resonance with localized states leads to the drastic conductance fluctuations in 1D systems [15–17], which is the case in regime II. This can also be gleaned from the highly nonlinear current-voltage (I-V) characteristics (Fig. 3b) of the system recorded in regime II. At a resonance peak ($V_g = 10.4$ V, marked by a circle in Fig. 3a), the I-V is only linear near zero bias and exhibits lower conductance at higher bias due to the larger energy window of the incident electrons and thus a larger fraction of off-resonance electrons. The shape of the I-V curve at the conductance peak (Fig. 3b) excludes CB physics for which linear I-V is expected at conductance peaks. The peak conductance increases as temperature decreases (Fig. 3a). This is due to the fact that at lower temperatures electrons are more "monochromatic" with smaller thermal broadening in energy. At a conductance valley ($V_g = 9.7$ V, marked by a square in Fig. 3a) in regime II, the I-V is also nonlinear, with higher conductance at high bias than near zero bias (Fig. 3b inset).

In regime II, the localized states strongly manifest as can be seen in the large conductance fluctuations and narrow peaks. They are much less pronounced in energy regimes I and III, where the slow conductance fluctuations relax to
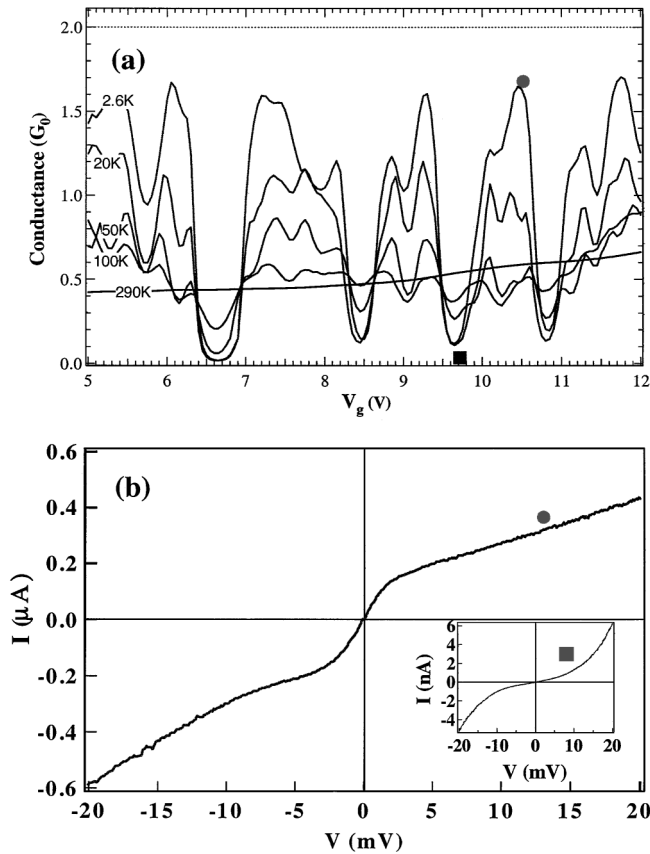
FIG. 3.   Manifestation of localized states. (a) Conductance vs gate-voltage curves recorded in regime II of Fig. 1a. (b) Nonlinear I-V curve recorded at a conductance peak marked in (a). Inset: I-V curve recorded at the valley marked in (a). The circle and square in (b) indicate the corresponding gate voltages in (a).

smaller amplitudes with broader peaks and larger spacing between the peaks. This is attributed to the energy dependent resonance effect, which is similar to an observation made recently in metallic SWNTs that the transparency of scattering sites depends on energy [20]. In energy regimes I and III, the electronic states in the nanotube can be characterized as more extended over the length of the tube, which allows the observation of an interference pattern with standing waves in the tube.

The existence of localized states points to imperfections in our nanotube sample. We can estimate the length scale of the localized states. In regime II, the conductance fluctuations have an average period of $\Delta V_g^I \sim 1.5$ V (Fig. 1). This corresponds to a Fermi energy change of $\Delta E \sim \alpha \Delta V_g^I = 75$ meV $\sim (dE/dk)\Delta k = h\upsilon_F/2L'$. Thus, the localized states can be roughly considered as confined in a length scale of $L' \sim 30$ nm. Unfortunately, it is not possible to identify the precise location of the defects on the nanotube. The bound states could be formed between a dominant defect close to one of the electrodes, or between two defects on the nanotube. Also not clear is the precise nature of the defects, although they are likely to be associated with chemical effects such as locally adsorbed molecule species (e.g., oxygen) [21–23]. This is based on the

thermal-cycle dependence of the conductance fluctuations (Fig. 1a vs 1b), which suggests that the defects responsible for the resonant localized states have a dependence on environmental factors.

Quantum interference effects are manifested by phase coherent electrons. At low temperatures, electron phase coherence in a nanotube is gained by the decrease in occupation numbers of phonon modes and thus reduced inelastic scattering. This is consistent with our observation of the average conductance increases as temperature decreases (Fig. 1). Such behavior has been seen in earlier studies of SWNTs, also attributed to phonon effect [24]. Reduced phonon occupations at low temperatures are indeed probed by heat capacity measurements [25]. However, the detailed behavior of conductance vs temperature depends on energy. For instance, at the valleys of slow conductance fluctuations in regime I or III, a downturn in conductance is observed below $T < 30$ K (Fig. 4a). Similar downturn behavior has been seen previously and attributed to localization effect [24]. At the peaks of the slow conductance fluctuations however, the resistance exhibits an upturn below 30 K (Fig. 4b) due to resonance effect, and has not been seen before. These results suggest that the full spectrum of conductance vs energy is important in understanding the electrical properties of nanotubes.

We point out that our results were obtained with an individual SWNT (diameter ~1.5 nm) instead of a bundle. The nanotube was grown under a low yield chemical vapor deposition process for producing isolated SWNTs [9]. Bundled SWNTs with diameter >3 nm were occasionally encountered in our samples and were excluded for measurements. Our results clearly show that two channels exist in a metallic SWNT for electron transport as predicted theoretically. The possible reasons for one-open channel and $G = 1G_0$ in a MWNT could be due to interlayer interactions [6] or an opaque π channel [7]. Experimental wise, our SWNTs were contacted by two symmetric transparent ($T \sim 1$) titanium electrodes. The MWNT was intimately contacted by liquid metal at one end, while the other end was coupled to other nanotubes in a bundle [6]. It could be possible that the intratube contact is nonideal and contributes to $G < 2G_0$.

With several low resistance SWNTs, we have observed resonance phenomena and conductance approaching $2G_0$ at certain gate voltages (Fig. 1b inset shows a second sample). For SWNTs with length <1 μm, we typically find that their maximum conductance can approach $2G_0 = 4e^2/h$. Several independent samples are observed exhibiting a dip in G vs V_g, and the details of the dip vary in different cooldowns. These results point to the fact that chemical species (e.g., oxygen) adsorbed on SWNTs could be a common cause for localized states that manifest as strong resonant scatters in a certain energy (dip) regime. Indeed, resonance effects due to chemisorbed oxygen atoms on SWNTs have been revealed theoretically [21]. Measurements of molecularly clean SWNTs will be desired and are currently underway. For nanotubes
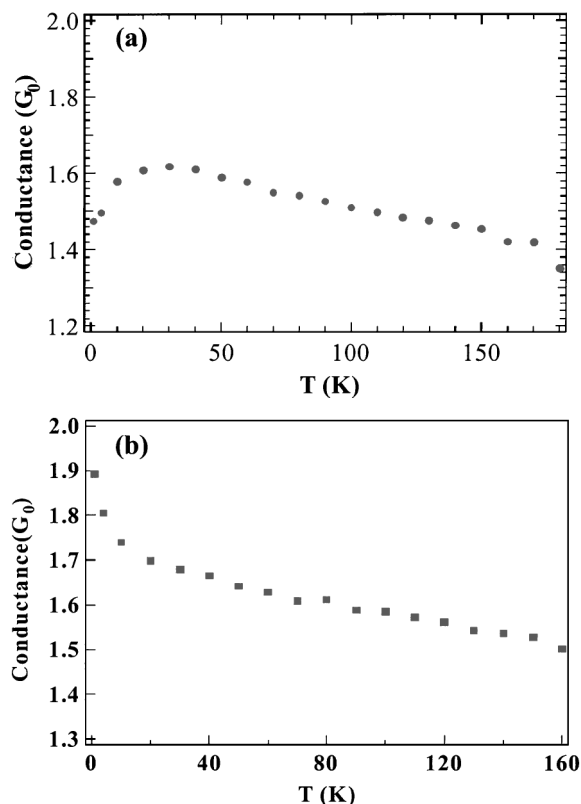
FIG. 4. Temperature dependent sample conductance depends on gate voltage. (a) G vs T for $V_g = -18$ V at a local conductance valley in regime III. (b) G vs T for $V_g = -16$ V at a local conductance peak in regime III.

with length on the order of $10-20$ μm, sharp and closely spaced conductance peaks are typically observed at 1.5 K, and the overall sample conductance turns lower below a certain temperature in the range of $50-20$ K. These results point to the higher probability of imperfections on $10-20$ μm long nanotubes, which can eventually lead to insulating systems due to localization [15]. Further effort is needed to elucidate the detailed nature and positions of defects and correlate them with transport properties of nanotubes.

[1] C. Dekker, Phys. Today **52**, No. 5, 22 (1999).
[2] C. T. White and T. N. Todorov, Nature (London) **393**, 240 (1998).
[3] S. J. Tans *et al.,* Nature (London) **386**, 474 (1997).
[4] M. Bockrath *et al.,* Science **275**, 1922 (1997).
[5] M. Bockrath *et al.,* Nature (London) **397**, 598 (1999).
[6] S. Frank, P. Poncharal, Z. L. Wang, and W. A. d. Heer, Science **280**, 1744 (1998).
[7] H. J. Choi, J. Ihm, Y. G. Yoon, and S. G. Louie, Phys. Rev. B **60**, 14 009 (1999).
[8] A. Bachtold *et al.,* Phys. Rev. Lett. **84**, 6082 (2000).
[9] H. Soh *et al.,* Appl. Phys. Lett. **75**, 627 (1999).
[10] J. Nygard, D. H. Cobden, and P. E. Lindelof, Nature (London) **408**, 342 (2000).
[11] Y. Zhang, N. Franklin, R. Chen, and H. Dai, Chem. Phys. Lett. **331**, 35 (2000).
[12] D. Chouvaev, L. S. Kuzmin, D. S. Golubev, and A. D. Zaikin, Phys. Rev. B **59**, 10 559 (1999).
[13] B. J. van Wees, L. P. Kouwenhoven, E. M. M. Willems, C. J. P. M. Harmans, and J. E. Mooij, Phys. Rev. B **43**, 12 431 (1991).
[14] Q. Wang *et al.,* Appl. Phys. Lett. **76**, 2274 (2000).
[15] P. A. Lee, Rev. Mod. Phys. **57**, 287 (1985).
[16] M. Y. Azebel, Solid State Commun. **45**, 527 (1983).
[17] A. B. Fowler, A. Hartstein, and R. A. Webb, Phys. Rev. Lett. **48**, 196 (1982).
[18] L. C. Venema *et al.,* Science **283**, 52 (1999).
[19] J. Kong, C. Zhou, E. Yenilmez, and H. Dai, Appl. Phys. Lett. **77**, 3977 (2000).
[20] M. Bockrath *et al.,* Science **291**, 283 (2001).
[21] A. Rochefort and P. Avouris, J. Phys. Chem. A **104**, 9807 (2000).
[22] J. Kong *et al.,* Science **287**, 622 (2000).
[23] P. G. Collins, K. Bradley, M. Ishigami, and A. Zettl, Science **287**, 1801 (2000).
[24] J. E. Fischer *et al.,* Phys. Rev. B **55**, R4921 (1997).
[25] J. Hone, B. Batlogg, Z. Benes, A. T. Johnson, and J. E. Fischer, Science **289**, 1730 (2000).